nature geoscience

LETTERS

PUBLISHED ONLINE: 23 SEPTEMBER 2012 | DOI: 10.1038/NGEO1585

Contributions to late Archaean sulphur cycling by life on land

Eva E. Stüeken*, David C. Catling and Roger Buick

Evidence in palaeosols suggests that life on land dates back to at least 2.76 Gyr ago[1,2]. However, the biogeochemical effects of Archaean terrestrial life are thought to have been limited, owing to the lack of a protective ozone shield from ultraviolet radiation for terrestrial organisms before the rise of atmospheric oxygen levels several hundred million years later[3]. Records of chromium delivery from the continents suggest that microbial mineral oxidation began at least 2.48 Gyr ago[4] but do not indicate when the terrestrial biosphere began to dominate important biogeochemical cycles. Here we combine marine sulphur abundance data with a mass balance model of the sulphur cycle to estimate the effects of the Archaean and early Proterozoic terrestrial biosphere on sulphur cycling. We find that terrestrial oxidation of pyrite by microbes using oxygen has contributed a substantial fraction of the total sulphur weathering flux since at least 2.5 Gyr ago, with probable evidence of such activity 2.7–2.8 Gyr ago. The late Archaean onset of terrestrial sulphur cycling is supported by marine molybdenum abundance data and coincides with a shift to more sulphidic ocean conditions[5]. We infer that significant microbial land colonization began by 2.7–2.8 Gyr ago. Our identification of pyrite oxidation at this time provides further support for the appearance[6] of molecular oxygen several hundred million years before the Great Oxidation Event.

We investigated sulphur abundances in marine sediments as a proxy for life on land, because the various mechanisms by which sulphur can be supplied or removed are understood well enough to detect biological contributions. Our database of ancient marine sedimentary sulphide concentrations (1,194 samples from 70 Precambrian formations) in fine-grained clastic facies was compiled from the literature. These data show (Supplementary Fig. S1) that significant increases in the relative abundance of sulphur occurred in the late Archaean and again after the rise in oxygen levels ~2.5 Gyr ago. Owing to scatter in the data, we employed statistical tests to verify our inferred trends to 95% confidence levels or better. The enrichment of sulphur relative to the siliciclastic background implies a selective enhancement of the sulphur input, which could have been caused by biotic or abiotic weathering, volcanic degassing or hydrothermal fluids. To evaluate the contributions of different sulphur sources, we constructed a sulphur cycle model.

In our model, the steady-state biogenic input of sulphur to the ocean (F_{bioticw}) is estimated as the difference between the total output (F_{out}) and the combined abiotic input fluxes after accounting for detrital sulphide deposition (Supplementary Fig. S2). Before the advent of widespread sulphate-rich evaporites late in the Proterozoic eon, the main sink for continent-derived sulphur is assumed to be precipitation of sulphide minerals in continental shelf environments, as it is now. Therefore, the total output flux for the earlier Precambrian time (F_{out}) can be calculated as the product of the sedimentation rate on continental shelves (D) and the concentration of sulphide in shelf sediments ([S]). We assume a sedimentation rate similar to modern, noting that a lower rate due to smaller or more inundated Archaean continents does not alter our ultimate conclusions (Supplementary Section S3.3). Abiotic input fluxes considered in the model include volcanic emissions (F_{volc}) and abiotic oxidative weathering (F_{abioticw}). We ignore hydrothermal sulphur (Supplementary Section S3.2) because it would have precipitated proximal to deep-sea vents under the anoxic conditions prevailing throughout the earlier Precambrian. Potential additions by detrital pyrite are accounted for by iteratively modifying the model on the basis of the assumption that negligible detrital sulphide was deposited after atmospheric oxygenation. We emphasize that increased erosion responsible for enhanced fluxes of detrital pyrite (perhaps because of continental growth) would have raised the total supply of clastic sediments without increasing the relative concentration of sulphur. Selective continental weathering of sulphide minerals can thus be monitored by comparing the average total sulphur concentration ([S]) between different stages. The volcanic flux is calculated following previously published parameterizations[7].

The model can be expressed through the following relationships:

$$F_{\mathrm{in}} = F_{\mathrm{out}} \Rightarrow F_{\mathrm{volc}} + F_{\mathrm{w}} = D \cdot [S] \Rightarrow F_{\mathrm{volc}} + (F_{\mathrm{abioticw}} + F_{\mathrm{bioticw}}) = D \cdot [S] \quad (1)$$

A detailed description of the computation of these individual fluxes and sensitivities to assumptions is given in the Supplementary Information. In brief, the abiotic oxidative weathering flux (F_{abioticw}) is a function of atmospheric oxygen levels, pH and the surface area of exposed sulphide minerals[8] (Supplementary Section S4.3). We assume 10^{-5} present atmospheric levels of oxygen in the Archaean eon and a generous 10^{-1} present atmospheric levels in the Proterozoic (ref. 9 and citations therein). Weathering pH is set to 7 and the surface area of exposed sulphide is calculated for modern conditions and held constant throughout the Precambrian. If pH were more acid (from release of sulphuric acid) or the area of abiotically weathered sulphide minerals were smaller in the Precambrian, a greater biotic flux is required to account for the total weathering sulphur flux (Supplementary Section S4.2). Thus, the pH and area assumptions are conservative.

The total continental sulphur weathering flux (F_{w}) through time inferred from the data is shown in Fig. 1. The dispersion in the fluxes at individual times probably arises from environmental

Department of Earth and Space Sciences and Astrobiology Program, University of Washington, Box 351310, Seattle, Washington 98195, USA.
*e-mail: evast@u.washington.edu.

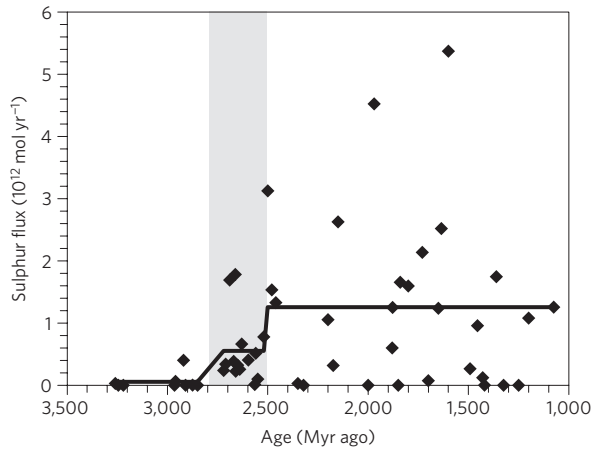

Figure 1 | Total inferred weathering flux F_w to continental margins over time. The values are calculated using equation (1). Each individual point at a given time is derived from averaged marine sulphur concentrations from one geologic formation or more if there are several formations of the same age. Calculated average fluxes for three temporal stages are shown as horizontal lines, where the stages are 2.5–1.0, 2.8–2.5 (shaded) and 3.3–2.8 Gyr ago.

differences between geological formations causing a spread in sulphur concentrations and from temporal or spatial variations in the sedimentation rate that are not accounted for by the model. To identify long-term changes in the weathering flux, we divide the data set into two, stepping through 100 Myr increments (Supplementary Section S5), and calculate the statistical significance of the difference between the two data blocks. Significant changes in the continental weathering flux of sulphur occur at 2.8 and 2.5 Gyr ago. Consequently, the sulphur weathering flux can be divided into three stages (Table 1). On average, $F_w(t)$ is required to increase by a factor of ~10.0 ($p_{one-tailed} = 0.003$) from the first Archaean stage (3.3–2.8 Gyr ago) to the second Archaean stage (2.8–2.5 Gyr ago), and then by a factor of ~2.3 ($p_{one-tailed} = 0.010$) from the second Archaean stage to the post-Archaean. If we compare the average $F_w(t)$ for all the Archaean data (>2.5 Gyr ago) to the Proterozoic (2.5–1.0 Gyr ago), we observe an increase across the Archaean–Proterozoic boundary by a factor of ~3.5 ($p_{one-tailed} = 0.001$).

Abiotic weathering alone cannot explain the total observed weathering flux at any stage (Fig. 2). The difference between total weathering and abiotic weathering before 2.8 Gyr ago may be explained by detrital sulphur input[10–12], but this cannot explain the increase in total weathering in the late Archaean and across the Archaean–Proterozoic boundary because both steps are accompanied by statistically significant increases in the total sulphur concentration in sediments (Supplementary Table S3). Enhanced erosion of land masses adding detrital sulphur would also have increased the flux of siliciclastic sediments, which does not preferentially enrich sulphur. It is possible that abiotic pyrite oxidation or degassing of very sulphur-rich volcanic rocks such as komatiites temporarily led to a higher sulphur input into the ocean than is accounted for by the model. Both scenarios can be tested using a compilation of molybdenum concentrations in clastic marine sediments over time (Fig. 3) because, unlike sulphur, Mo is not volatile and is uniformly distributed between ultramafic to felsic rocks[13,14]. After averaging data for each time point and then for different time periods, we see significant increases in sedimentary Mo concentrations around 2.7 Gyr ago by a factor of 2.1 ($p_{one-tailed} = 0.003$) and again around 2.5 Gyr ago by a factor of 5.7 ($p_{one-tailed} = 0.01$). A division of the Mo data set at 2.8 Gyr ago is also statistically significant ($p_{one-tailed} = 0.02$). Therefore, the increases in the total sulphur weathering flux observed at those times can be explained only by oxidation of continental sulphides. As abiotic weathering has already been accounted for, these results imply that biological oxidation ($F_{bioticw}(t)$) has dominated the flux of sulphur to continental shelves since 2.5 Gyr ago and probably 2.8 Gyr ago. The record of sulphur concentrations in clastic marine sediments thus provides strong evidence for an extensive terrestrial biosphere since the Great Oxidation Event (GOE) and most probably earlier.

This conclusion is consistent with sulphur isotopes (Supplementary Fig. S3) indicating oxidative weathering since ~2.8 Gyr ago or shortly thereafter[15], as well as with authigenic Cr enrichments indicating a biogenic chromium flux from continents to the ocean at ~2.4 Gyr ago[4] (Supplementary Fig. S10). The absence of Cr enrichments before 2.4 Gyr ago is probably due to the higher redox potential of Cr relative to S and hence a difference in sensitivity between the two proxies. Enhanced late Archaean continental weathering can also be reconciled with the record of increasing mass-independent fractionation (MIF) of sulphur isotopes in the late Archaean (for example, ref. 16). As MIF is produced by photolysis reactions, the MIF record suggests incorporation of atmospherically processed sulphur, which is usually considered to be volcanogenic SO_2 or H_2S. If, however, biotic continental weathering were more important than previously supposed and exceeded the volcanic input to shelf sediments (Fig. 2), then our results may be evidence that a greater flux of biogenic sulphur gases such as CS_2 or dimethyl sulphide to the late Archaean atmosphere contributed significantly to the preservation of MIF (ref. 17).

It is generally thought that the lack of an atmospheric ozone shield before the GOE resulted in lethal ultraviolet radiation on Earth's land surface, preventing the colonization of terrestrial habitats (for example, ref. 3). However, a Precambrian terrestrial biosphere may have thrived in endolithic habitats, such as those found in Antarctica today[18], and was clearly present in Archaean lakes such as those of the Tumbiana Formation by 2.72 Gyr ago[19]. Alternatively, an organic haze derived from methane photolysis may have provided some ultraviolet shielding[20,21]. If a terrestrial biota was already extensive in the late Archaean between 2.8 and 2.5 Gyr ago, then expansion out of local, protected habitats onto exposed

Table 1 | Average sulphur fluxes to continental shelves.

	F_{volc}	F_w	$F_{abioticw}$	$F_{bioticw}$
3.3–2.8 Gyr ago	1.3×10^{11} (70.4%)	5.5×10^{10}	3.5×10^{9} (1.9%)	5.2×10^{10} (27.7%)
2.8–2.5 Gyr ago	1.2×10^{11} (17.6%)	5.5×10^{11}	3.5×10^{9} (0.5%)	5.5×10^{11} (81.9%)
>2.5 Gyr ago	1.2×10^{11} (25.8%)	3.6×10^{11}	3.5×10^{9} (0.7%)	3.5×10^{11} (73.4%)
2.5–1.0 Gyr ago	9.2×10^{10} (6.9%)	1.3×10^{12}	3.5×10^{11} (26.0%)	9.0×10^{11} (67.1%)
Modern	6.0×10^{10} (2.9%)*	2.0×10^{12} †	1.1×10^{12} (53.7%)	9.0×10^{11} (43.4%)

Values are reported in moles per year. See the text for definitions of F_{volc}, F_w, $F_{abioticw}$ and $F_{bioticw}$. Relative contributions of sulphur sources to continental shelf sediments are given in parentheses, noting that there are considerable inferred increases in the absolute total weathering fluxes in the Proterozoic and Phanerozoic. *From ref. 7 and references therein, scaled by 30% to account for the fraction deposited on continental shelves (see the main text). †Total river flux (4.03×10^{12} mol yr^{-1} from ref. 28) scaled by 50% to include only the natural pyrite-derived fraction.

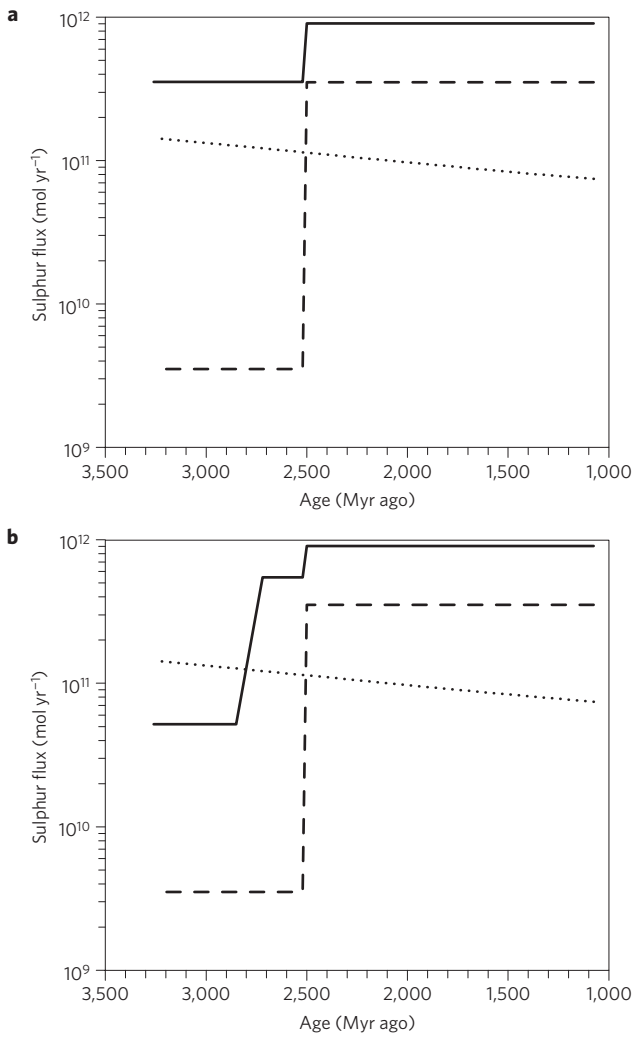

Figure 2 | Contribution of different sulphur sources to continental margin sediments. a, The data contributing to the calculations have been divided up into two temporal stages of Archaean (>2.5 Gyr ago) and post-Archaean (2.5–1.0 Gyr ago). **b**, The data have been divided up into three temporal stages: 3.3–2.8, 2.8–2.5 and 2.5–1.0 Gyr ago. The solid line marks the biotic/detrital weathering flux, the dashed line marks the abiotic weathering flux and the dotted line marks the volcanic flux; the various fluxes sum to the solid line shown in Fig. 1. It is evident that only a biotic weathering flux can account for the Proterozoic total weathering flux.

land areas after the rise of oxygen and coincident establishment of an ozone shield could explain the stepwise increase in the biogenic sulphur weathering flux from the late Archaean to the Proterozoic (Fig. 2). The inferred lower weathering flux of sulphur during the Proterozoic of $\sim 1.3 \times 10^{12}$ mol yr^{-1} compared with the modern $\sim 2.0 \times 10^{12}$ mol yr^{-1} (Table 1) implies further expansion of terrestrial life in the late Neoproterozoic era or the Phanerozoic eon. Mid-Proterozoic atmospheric oxygen levels were probably between 1% and ~10% of the present[22], and under such conditions, biotic pyrite oxidation as well as aerobic heterotrophy may have been less effective energy sources than today. Our results may therefore provide further evidence for a second rise of atmospheric oxygen levels in the Neoproterozoic. They are also consistent with carbon and oxygen isotope evidence for more efficient oxidation of terrestrial organic matter after 850 Myr ago (ref. 23).

Colonization of land masses by pyrite-oxidizing bacteria would also have affected marine life. By increasing the supply of sulphate, life on land would have allowed the ancient[24], but

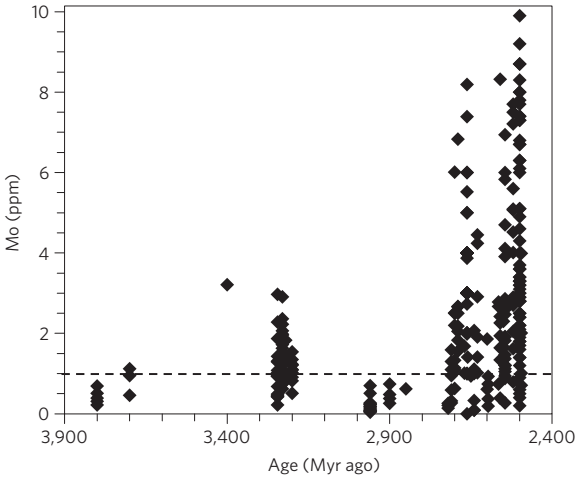

Figure 3 | Molybdenum concentrations in the late Archaean and early Proterozoic. The data show a step change around ~2.7 Gyr ago, which is significant to a 99% confidence level. References and further data are provided in Supplementary Section S6. The dashed black line marks the crustal average. Data from the Mount McRae Shale (2.5 Gyr ago) are cut off at 10 ppm.

previously suppressed[25], metabolism of dissimilatory sulphate reduction to become ecologically prominent in the ocean. Thus, the terrestrial biosphere would have been indirectly responsible for the widespread occurrence of euxinia along late Archaean and Proterozoic continental margins[26]. If microbial sulphate reduction suppressed methanogenesis, then the biotic weathering flux may also have facilitated the rise of oxygen in the atmosphere[9].

The advent of terrestrial biotic sulphide oxidation apparent by 2.8 Gyr ago and certain by 2.5 Gyr ago implies that a significant source of oxidants was available, most likely biogenic O_2 (Supplementary Section S4.3). The large biotic weathering flux derived in our model requires an O_2 source of similarly large magnitude, possibly in close spatial proximity. As only cyanobacteria are known to generate O_2 in large quantities during their metabolism, our results may provide indirect evidence for the Archaean evolution of these microbes and indicate that the appearance of oxygenic photosynthesis preceded the GOE by at least several hundred million years (contradicting ref. 27). This joins several other lines of evidence supporting such a conclusion (summarized by ref. 6) and implies that atmospheric oxygenation was retarded by geological oxygen sinks.

We conclude that continents have been inhabited by microbial communities since at least 2.5 Gyr ago and probably 2.8 Gyr ago, and their metabolic activity played a significant role in the global biogeochemical cycles of redox-sensitive elements, particularly sulphur.

Received 11 July 2012; accepted 17 July 2012; published online 23 September 2012

References

1. Rye, R. & Holland, H. D. Life associated with a 2.76 Ga ephemeral pond?: Evidence from Mount Roe #2 paleosol. *Geology* **28,** 483–486 (2000).
2. Watanabe, Y., Martini, J. E. J. & Ohmoto, H. Geochemical evidence for terrestrial ecosystems 2.6 billion years ago. *Nature* **408,** 574–578 (2000).
3. Cockell, C. S. The ultraviolet history of the terrestrial planets - implications for biological evolution. *Planet. Space Sci.* **48,** 203–214 (2000).
4. Konhauser, K. O. *et al.* Aerobic bacterial pyrite oxidation and acid rock drainage during the Great Oxidation Event. *Nature* **478,** 369–373 (2011).
5. Reinhard, C. T., Raiswell, R., Scott, C. T., Anbar, A. & Lyons, T. W. A late Archean sulfidic sea stimulated by early oxidative weathering of the continents. *Science* **326,** 713–716 (2009).
6. Buick, R. When did oxygenic photosynthesis evolve? *Phil. Trans. R. Soc. B* **363,** 2731–2743 (2008).

7. Canfield, D. E. The evolution of the Earth surface sulfur reservoir. *Am. J. Sci.* **304,** 839–861 (2004).
8. Williamson, M. A. & Rimstidt, J. D. The kinetics and electrochemical rate-determining step of aqueous pyrite oxidation. *Geochim. Cosmochim. Acta* **58,** 5443–5454 (1994).
9. Catling, D. C. & Claire, M. W. How Earth's atmosphere evolved to an oxic state: a status report. *Earth Planet. Sci. Lett.* **237,** 1–20 (2005).
10. England, G. L., Rasmussen, B., Krapez, B. & Groves, D. I. Palaeoenvironmental significance of rounded pyrite in siliclastic sequences of the Late Archaean Witwatersrand Basin: Oxygen-deficient atmosphere or hydrothermal alteration? *Sedimentology* **49,** 1133–1156 (2002).
11. Rasmussen, B. & Buick, R. Redox state of the Archean atmosphere: evidence from detrital heavy minerals in ca. 3250–2750 Ma sandstones from the Pilbara Craton, Australia. *Geology* **27,** 115–118 (1999).
12. Holland, H. D. When did the Earth's atmosphere become oxic? A Reply. *Geochem. News* **100,** 20–22 (1999).
13. Taylor, S. R. Abundance of chemical elements in the continental crust: a new table. *Geochim. Cosmochim. Acta* **28,** 1273–1285 (1964).
14. Eggins, S. M. *et al.* A simple method for precise determination of >40 trace elements in geological samples by ICPMS using enriched isotope internal standardisation. *Chem. Geol.* **134,** 311–326 (1997).
15. Strauss, H. in *Precambrian Sedimentary Environments: A Modern Approach to Ancient Depositional Systems* (eds Altermann, W. & Corcoran, P. L.) (Blackwell Science, 2002).
16. Farquhar, J. *et al.* Isotopic evidence for Mesoarchaean anoxia and changing atmospheric sulphur chemistry. *Nature* **449,** 706–709 (2007).
17. Zahnle, K. J., Claire, M. W. & Catling, D. C. The loss of mass-independent fractionation in sulfur due to a Palaeoproterozoic collapse of atmospheric methane. *Geobiology* **4,** 271–283 (2006).
18. Walker, J. J. & Pace, N. R. Endolithic microbial ecosystems. *Annu. Rev. Microbiol.* **61,** 331–347 (2007).
19. Buick, R. The antiquity of oxygenic photosynthesis: Evidence from stromatolites in sulphate-deficient Archean lakes. *Science* **255,** 74–77 (1992).
20. Pavlov, A. A., Brown, L. L. & Kasting, J. F. UV shielding of NH_3 and O_2 by organic hazes in the Archean atmosphere. *J. Geophys. Res.* **106,** 23267–23287 (2001).
21. Wolf, E. T. & Toon, O. B. Fractal organic haze provided an ultraviolet shield for early earth. *Science* **328,** 1266–1268 (2010).
22. Canfield, D. E. The early history of atmospheric oxygen: Homage to Robert M. Garrels. *Annu. Rev. Earth Planet. Sci.* **33,** 1–36 (2005).
23. Knauth, L. P. & Kennedy, M. J. The late Precambrian greening of the Earth. *Nature* **460,** 728–732 (2009).
24. Shen, Y., Buick, R. & Canfield, D. E. Isotopic evidence for microbial sulphate reduction in the early Archaean era. *Nature* **410,** 77–81 (2001).
25. Habicht, K. S., Gade, M., Thamdrup, B., Berg, P. & Canfield, D. E. Calibration of sulfate levels in the Archean Ocean. *Science* **298,** 2372–2374 (2002).
26. Poulton, S. W. & Canfield, D. E. Ferruginous conditions: A dominant feature of the ocean through Earth's history. *Elements* **7,** 107–112 (2011).
27. Liang, M-C., Hartman, H., Kopp, R. E., Kirschvink, J. L. & Yung, Y. L. Production of hydrogen peroxide in the atmosphere of a Snowball Earth and the origin of oxygenic photosynthesis. *Proc. Natl Acad. Sci. USA* **103,** 18896–18899 (2006).
28. Emerson, S. & Hedges, J. *Chemical Oceanography and The Marine Carbon Cycle* (Cambridge Univ. Press, 2008).

Acknowledgements

We thank H. Strauss for sharing his sulphur database. This study was financially supported by NSF EAR-0921580. D.C.C. also acknowledges support from NASA Astrobiology grant NNX10AQ90G and the NAI Virtual Planetary Laboratory.

Author contributions

E.E.S. and D.C.C. designed and analysed the model, and all authors contributed to the collection of literature data and the composition of the manuscript.

Additional information

Supplementary information is available in the online version of the paper. Reprints and permissions information is available online at www.nature.com/reprints. Correspondence and requests for materials should be addressed to E.E.S.

Competing financial interests

The authors declare no competing financial interests.

nature geoscience

SUPPLEMENTARY INFORMATION

DOI: 10.1038/NGEO1585

Contributions to Late Archaean sulphur cycling by life on land

Eva E. Stüeken[1,*], David C. Catling[1], Roger Buick[1]

1. University of Washington, Department of Earth & Space Sciences and Astrobiology Program, Box 351310, Seattle, WA-98195, US

S1. Sulphur data sources

Data sources are shown in Table S1 where formation ages were revised where conflicts or discrepancies occurred. All data points are provided in a separate excel file. We used total sulphur concentrations, unless the total sulphide fraction was specifically reported, assuming that sulphate contributions are negligible or small throughout that part of the Precambrian considered here, prior to 1.0 Gyr.

For each age point, outliers defined as larger or smaller than the average +/- two standard deviations were removed from the dataset. It is possible that post-depositional effects led to addition or removal of sulphur in individual samples; however, this would apply to sediments of any age. Thus by taking long-term averages of many data points, effects of post-depositional alteration become minimal.

Table S1: Data sources for sulphur concentrations from Precambrian shales

Age [Myr]	Location	Author	Age revised after
1075	Nonesuch Shale	1	
1200	Borden Basin	2	
1250	Hongshuizhuang Fm	3	
1325	Wumishan Fm	3	
1361	Velkerri Fm	4	5
1361	Velkerri Fm	6	5
1361	Velkerri Fm	2	5
1361	Lansen Creek Shale	7	5
1361	Velkerri Fm	7	5
1420	Greyson Fm	3	
1429	McMinn Fm	7	8
1429	Corcoran Fm	7	8
1429	Mainoru Fm	7	8
1455	Newland Fm	9	
1455	Newland Fm	3	
1455	Prichard Fm	3	
1600	Bijaigarh Shale	10	

1600	Rampur Shale	10	
1635	Reward Fm	11	8
1650	Candlow Fm	7	
1700	Deoland Fm	10	
1700	Kajrahat Fm	10	
1730	Wollogorang Fm	11	
1700	Chuanlingguo Fm	3	12
1800	Temiscamie Fm	13	14
1800	Albanel Fm	13	14
1840	Rove Fm	15	
1840	Rove Fm	13	15
1850	Whitewater Fm	13	16
1878	Gunflint Fm	13	17
1880	Menihek Fm	13	18
1880	Ruth Shale	13	19
1880	Fontano Fm	3	20
1880	Attikamagen Group	13	19
1970	Pilgujarvi Fm	21	22
2000	Whites Fm	7	
2150	Francevillian Series	2	
2150	Sengona Argillite Fm	2	
2150	Zaonezhskaya Fm	2	
2174	Silverton Fm	23	24
2200	Mapedi Shale	25	26
2200	Mapedi Shale	7	26
2200	Mapedi Shale	26	
2322	Timeball Hill Fm	23	27
2322	Timeball Hill Fm	26	27
2350	Gowganda Fm	13	28
2460	Malips Mbr, Penge Fm	29	30
2480	Dales Gorge Mbr	29	31
2500	Mt McRae Shale	32	
2500	Mt McRae Shale	33	
2500	Mt McRae Shale	7	
2520	Klein Naute Fm	34	31
2520	Gamohaan Fm	2	35
2550	Oak Tree Fm	26	36
2550	Reivilo Fm	25	36
2550	Reivilo Fm	7	36
2560	Monteville Fm	37	36
2560	Monteville Fm	25	36
2560	Monteville Fm	7	36
2565	Wittenoom Dolomite Fm	38	39
2565	Wittenoom Dolomite Fm	26	39
2597	Marra Mamba Iron Fm	38	39
2597	Marra Mamba Iron Fm	26	39

2630	Carawine Dolomite Fm	38	40
2630	Carawine Dolomite Fm	26	8
2640	Black Reef Fm	25	26
2640	Black Reef Fm	7	26
2640	Black Reef Fm	23	26
2640	Black Reef Fm	26	
2650	Lokammona Fm	37	31
2650	Lokammona Fm	25	31
2650	Lokammona Fm	7	31
2660	Boomplaas Fm	25	31
2660	Boomplaas Fm	7	31
2662	Jeerinah Fm	38	2
2662	Jeerinah Fm	41	2
2662	Jeerinah Fm	33	2
2662	Jeerinah Fm	2	
2662	Jeerinah Fm	42	2
2662	Jeerinah Fm	3	2
2662	Jeerinah Fm	7	2
2662	Jeerinah Fm	26	2
2670	Vryburg Fm	37	31
2670	Vryburg Fm	25	31
2670	Vryburg Fm	7	31
2690	Lewin Shale	7	26
2690	Lewin Shale	26	
2710	Rietgat Fm	26	
2720	K-8	23	
2720	Pillingini Tuff Fm	26	
2850	Upper Jeppestown Shale	7	
2850	Lower Jeppestown Shale	7	
2850	Upper Government Shale	7	
2850	Middle Government Shale	7	
2850	Government Magnetic Shale	7	
2850	Lower Government Shale	7	
2850	Upper Coronation Shale	7	
2850	Middle Coronation Shale	7	
2850	Lower Coronation Shale	7	
2850	Observatory Shale	7	
2875	Booysens Shale	7	43
2875	Booysens Shale	23	43
2910	Roodepoort	23	
2920	Mosquito Creek Fm	44	
2960	Parktown Fm	26	
2965	Mozaan Gp	45	

2965	Mozaan Gp	7	45
3245	Sheba Fm	46	
3245	Sheba Fm	7	47
3245	Sheba Fm	26	47
3220	Moodies Gp	7	48
3260	Swartkoppie Fm	7	49

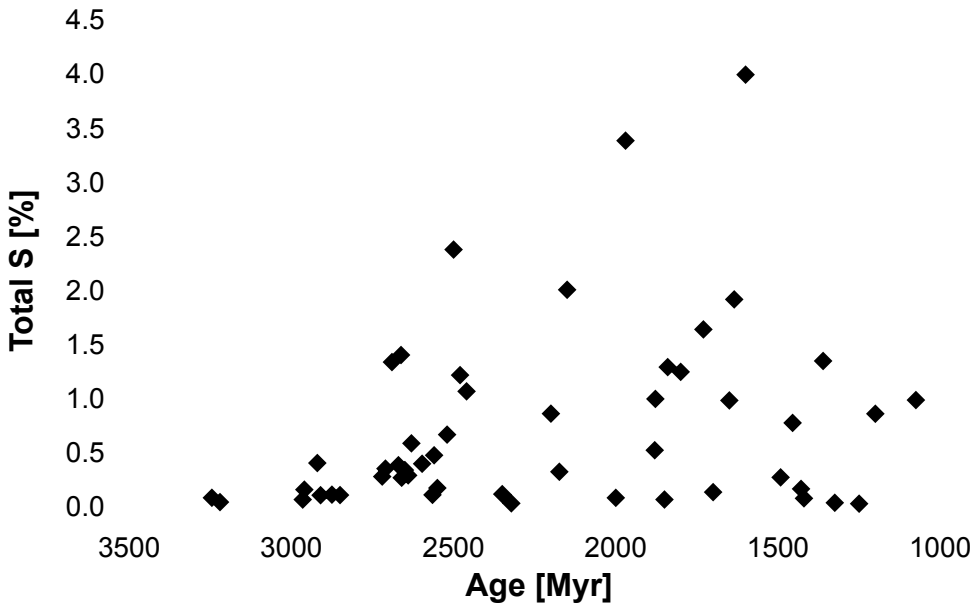

Fig. S1: Time-point average sulphur concentrations. For references see Table S1.

S2. Detailed Model Description

The major fluxes in and out of the ocean considered in the model are the total output flux F_{out}, and three input fluxes (Fig. S2): volcanic emission F_{volc}, abiotic oxidative weathering $F_{abioticw}$, and detrital + biological weathering $F_{bioticw}$. The sum of the latter two fluxes is the total weathering flux, F_w.

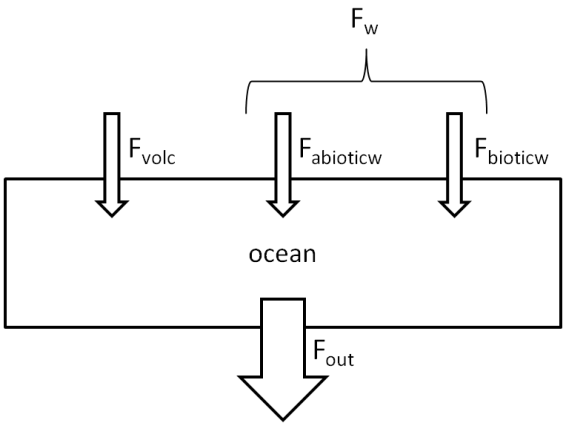

Fig. S2: A schematic diagram showing the basic sulphur fluxes considered in the model. See the text for definitions of the flux variables.

S2.1. Sulphur concentrations as a record of weathering fluxes

On timescales exceeding the residence time of sulphur, which would be shorter in the early ocean than today's 7.9 Myr (ref. 50) because of lower marine sulphate concentrations, it is reasonable to assume that the ocean attains steady state with respect to sulphur sources (F_{in}) and sinks (F_{out}) at any time t. Thus,

$$F_{in}(t) = F_{out}(t) \quad \text{(S1)}$$

Hereafter, we specify all fluxes in units of mol yr^{-1}.

S2.1.1. Sinks

On the modern Earth, shelf environments represent by far the largest sink for marine sulphur[51]. Farquhar *et al.*[52] estimated that throughout the Archaean and Paleoproterozoic essentially all continent-derived sulphur was deposited on continental shelves. We therefore assume that shelf sediments accurately record changes in the sulphur weathering flux over time. This assumption is conservative because it may lead to an underestimation of the total weathering flux in the Mesoproterozoic, if sinks to the deep ocean became important at that time.

Today, sulphur is lost from the ocean in the form of either sulphate evaporites or sulphide minerals. Data shows that marine sulphate concentrations were low until a second rise of oxygen in the Neoproterozoic[53,54] so that evaporite formation only became significant during that era[55]. However, the relative proportions of sulphide minerals and sulphate evaporites formed at any given time since then are poorly constrained. We therefore restrict our model to the Archaean, Paleo-, and Meso-proterozoic. During these times, the formation of sulphate evaporites can be neglected as a sink of sulphur from the ocean. This is also a conservative assumption because by neglecting sulphate evaporites as an additional sink we may underestimate the total weathering flux. But this simplification allows us to use sulphide concentrations of clastic shelf sediments to calculate the total sink, as follows:

$$F_{out}(t) = D \cdot [S](t) \quad \text{(S2)}$$

Here, D is the average rate of sedimentation on continental margins. We take a nominal, uniformitarian value of $D = 4.4 \cdot 10^{15}$ g yr^{-1}, which is the average sedimentation rate on continental margins during the Phanerozoic[56]. Sensitivity studies show that lower values of D, possibly due to smaller continents in the past, do not affect our conclusions (Supplementary Section S3.3 and S4.1). $[S](t)$ is the concentration of reduced sulphur in shelf sediments at time t. Sulphur concentrations are taken from an extensive database compiled from the literature of 1194 individual samples spread throughout 70 geologic formations (Supplementary Section S2). Only marine shales and siltstones are considered, because those represent the major lithologies on continental shelves today and probably also in the past[57]. Furthermore, coarser-grained facies are most likely to contain detrital sulphides that bypassed continental weathering (particularly prior to atmospheric oxygenation).

S2.1.2. Sources

Sulphur deposited on continental shelves is ultimately derived from either volcanic degassing ($F_{volc}(t)$) or continental weathering ($F_w(t)$) such that:

$$F_{in}(\mathrm{t}) = F_{volc}(\mathrm{t}) + F_w(\mathrm{t}) \quad \text{(S3)}$$

Contributions from hydrothermal vents can be neglected because evidence suggests that the Precambrian deep ocean was ferruginous[58] so that sulphur would have been locally removed as sulphide precipitates near the hydrothermal source (Supplementary Section S3.2). The volcanic sulphur flux is estimated by multiplying the modern flux ($F_{volc}(mod) = 2 \cdot 10^{11}$ mol yr^{-1}, ref. 59 and citations therein) by a factor Q which accounts for increased ancient volcanic activity. We take a parameterization of Q from Canfield[59], where $Q(t) = 1.00 + 0.1217 \cdot \mathrm{t} + 0.0942 \cdot \mathrm{t}^2$. Here t is the age in billion years ago (Gyr) (Supplementary Section S3.1). Thus:

$$F_{volc}(t) = F_{volc}(mod) \cdot Q(t) \cdot f_{cont} \quad \text{(S4)}$$

where f_{cont} is the fraction of the Earth's surface area covered by continents. For example, if f_{cont} was similar in the Archaean to the modern value, only approximately 30 % of the volcanic sulphur would have been deposited on continental shelves at any given time, while the remaining 70 % would have been incorporated into deep-sea sediments. Therefore the volcanic flux of sulphur reaching shelf sediments would be scaled by a factor of $f_{\mathrm{cont}} = 0.3$. The assumption of a modern value for f_{cont} is conservative for our purposes because it leads to an underestimation if continents were smaller in the Precambrian (cf. ref. 60).

The total continental weathering flux $F_w(\mathrm{t})$ is then calculated as the difference between the total sink (Eq. S2) and the volcanic flux (Eq. S4) (see the schematic in Fig. S2) such that:

$$F_w(t) = D \cdot [S](t) \; - \; F_{volc}(t) \quad \text{(S5)}$$

Using sulphur concentration data [S] from the literature (Table S1), we can calculate $F_w(t)$ using Eqn. (S5) (Fig. 1). If the product of D and [S](t) is smaller than $F_{volc}(t)$ due to exceptionally small concentrations of sulphur in a particular formation, Eq. (S5) gives the unrealistic result that the weathering flux $F_w(t)$ could be negative. We have excluded such unreasonable data points for a few very sulphur-poor formations by setting $F_w(t)$ in these cases to zero mol yr^{-1}.

Now that we have estimates of the flux of weathered sulphur from the continents, we assess whether this flux can be explained by purely abiotic weathering or must be explained by a larger biotic weathering flux.

S2.2. Weathering Sources

Sulphur liberated during continental weathering can have three source fluxes: abiotic oxidative weathering ($F_{abioticw}(t)$), mechanically weathered detrital pyrite, and biogenic weathering. We combine the last two fluxes into one variable ($F_{bioticw}(t)$) because they cannot be constrained independently. Hence,

$$F_w(t) = F_{abioticw}(t) + F_{bioticw}(t) \quad \text{(S6)}$$

S2.2.1. Abiotic weathering

Williamson and Rimstidt[61] experimentally determined a rate law for abiotic weathering of pyrite as a function of dissolved oxygen. In units of mol m^{-2} yr^{-1}, their abiotic pyrite oxidation rate (R_{pO2}) as a function of pO_2 (in units of atm) is:

$$R_{pO2} = 10^{-8.19(\pm 0.10)} \cdot ((p_{O2} \cdot K_{O2})^{0.5(\pm 0.04)}) / (m_{H+}{}^{0.11(\pm 0.01)}) \cdot 31{,}536{,}000 \quad \text{(S7)}$$

Here, K_{O2} is the Henry's law constant for O_2, which is 0.00126 mol L^{-1} atm^{-1} at 25°C (ref. 62), and 31,536,000 is a conversion factor from per second to per year. The molarity (mol L^{-1}) of protons is m_{H+}, *i.e.* the abiotic oxidation rate increases with decreasing m_{H+}, which is equivalent to increasing pH. In our model, we take a nominal pH of 7 for the weathering solution. Lower

pH values might occur in pyrite-rich settings because of the generation of acidity during sulphide weathering (ref 63, also reviewed in ref.64). Since our aim is to assess the relative importance of biotic versus abiotic weathering, we choose a conservative assumption (Supplementary Section S4.3). The partial pressure of oxygen is set to 10^{-5} times the present atmospheric level (PAL, 0.21 atm) for the Archaean and 10^{-1} PAL for the Proterozoic based on geologic constraints (*e.g.* ref. 65 and citations therein). The flux of abiotically weathered pyrite in units of mol-S yr^{-1} is then equal to the abiotic weathering rate (Eq. S7) multiplied by the total surface area of exposed pyrite (A_{py}):

$$F_{abioticw}(t) = A_{py} \cdot R_{po2}(t) \quad \text{(S8)}$$

We estimate A_{py} for the modern Earth, assuming initially that all pyrite weathered today is oxidized abiotically (Supplementary Section S3.2). This assumption is modified iteratively in subsequent steps (Supplementary Section 2.2.2), when an estimate of the biotic flux is made. To start with, we use the modern flux of riverine sulphate to the ocean ($F_w(mod) = 4.025 \cdot 10^{12}$ mol yr^{-1}) (ref. 66) divided by R_{po2} at 1 PAL:

$$A_{py} = F_w(mod) \cdot 0.5 / R_{po2}(mod) \quad \text{(S9)}$$

Berner and Berner[51] estimated that today more than 40 % of riverine sulphate is anthropogenic. Of the naturally produced sulphate, two thirds are likely derived from the dissolution of evaporites and only one third from the oxidation of sulphide minerals, but these relative proportions are poorly constrained. We therefore scale the modern flux $F_w(mod)$ by a conservative factor of 0.5 (Eq. S9).

S2.2.2. Biotic and physical weathering

The detrital plus biogenic sulphur flux ($F_{bioticw}(t)$) to continental shelves is calculated as the difference between the total weathering flux ($F_w(t)$) and the abiotic flux ($F_{abioticw}(t)$):

$$F_{bioticw}(t) = D \cdot [S](t) \; - \; F_{volc}(t) \; - \; A_{py} \cdot R_{po2}(t) \qquad \text{(S10)}$$

Detrital pyrite largely disappears from the geologic record after 2.3 Gyr because it dissolves in oxygenated river waters (reviewed in ref. 67). Hence the post-Archaean value for $F_{bioticw}(t)$ likely only comprises biogenic sulphur. The average Paleo- and Meso-Proterozoic biogenic sulphur flux are then subtracted from the modern flux ($F_w(mod)$) to obtain a more accurate estimate of the modern abiotic flux ($F_{abioticw}(mod)$). This value is then used iteratively to replace $F_w(mod)$ in Eq. S9 to calculate a new value for A_{py}. Convergence of Proterozoic $F_{bioticw}(t)$ to one decimal is achieved in five iterations. We then calculate long-term averages (Fig. 2), which is appropriate for two reasons. First, it is likely that the sedimentary sulphur concentrations reported in the literature represent a wide range of different environmental settings (*e.g.* Supplementary Section S3). Second, the exact nature of the evolution curve for atmospheric pO_2 over time is not well resolved.

S3. Possible biases in the total weathering flux

Several factors that our model does not account for could theoretically affect the total weathering flux calculated as $F_w(t) = D \cdot [S](t) - F_{volc}(t)$.

S3.1. Volcanic degassing

It is likely that the volcanic sulphur flux was variable over time and did not follow the smooth pattern prescribed by the Q-factor (Eq. S4). Such variations may contribute to the scatter in $F_w(t)$ (Fig. 1). By averaging over several hundred million years, the effects of periods with exceptionally low or high volcanic sulphur fluxes are reduced. Furthermore, the volcanic flux is generally minor compared to the total weathering fluxes, especially in the late Archaean and

Proterozoic (Fig. 2). Hence inaccuracies in our approximation of $F_{volc}(t)$ should not undermine the predominance of $F_w(t)$.

S3.2. Hydrothermal sulphur addition

We neglect hydrothermal addition to sedimentary sulphur because the very deep ocean was certainly ferruginous in the Archaean[46] and likely remained so until the end of the Mesoproterozoic[12,58], thus removing sulphide generated in deep-sea hydrothermal vents via pyrite precipitation. Consequently, hydrothermal sulphides would not have reached continental shelves. If hydrothermal sulphides had played a significant role, this assumption would result in an overestimate of $F_w(t)$. But there are additional reasons why this can be discounted. Most sedimentary sulphides of Proterozoic and late Archaean age show non-zero $\delta^{34}S$ values (Fig. S3) and a wider spread (Fig. S4) suggestive of bacterial sulphate reduction and thus predominance of non-hydrothermal sulphide. We cannot rule out the possibility of hydrothermal addition before 3 Gyr when $\delta^{34}S$ shows much less variation, though this was probably due to low concentrations of sulphate in the water column[68]. However, lastly, the total hydrothermal flux of sulphur into the ocean is equal to only about one third of the volcanic flux[59]. Since the volcanic flux is overall small compared to $F_w(t)$ (Fig. 2), hydrothermal input would not, if present, significantly affect our calculations or conclusions.

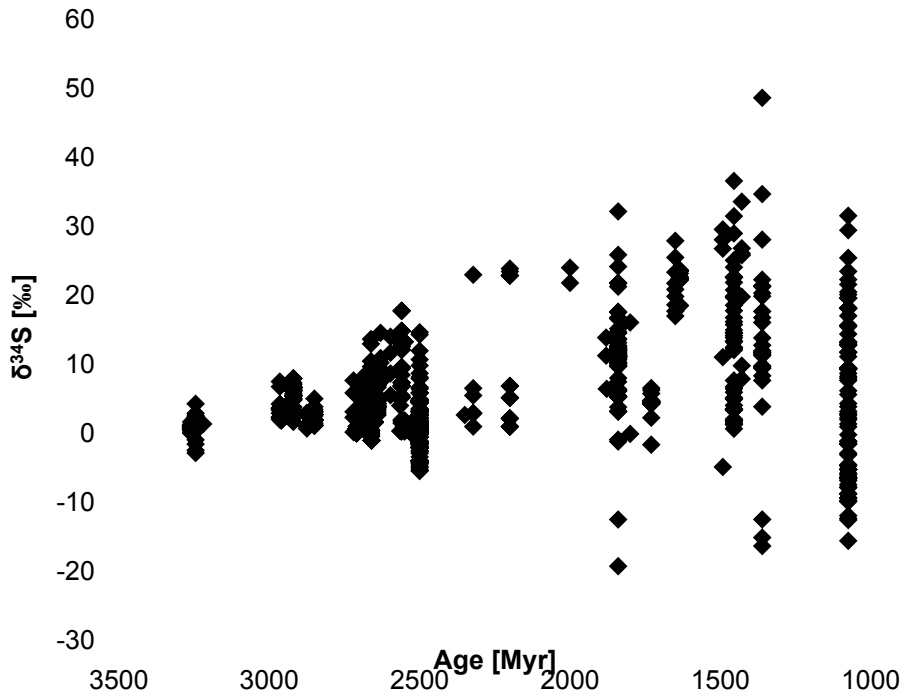

Fig. S3: Sulphur isotope compositions of data used in this model. See Table S1 for references. Note difference to Fig. S12 which includes data from other lithologies and environments not considered in this model.

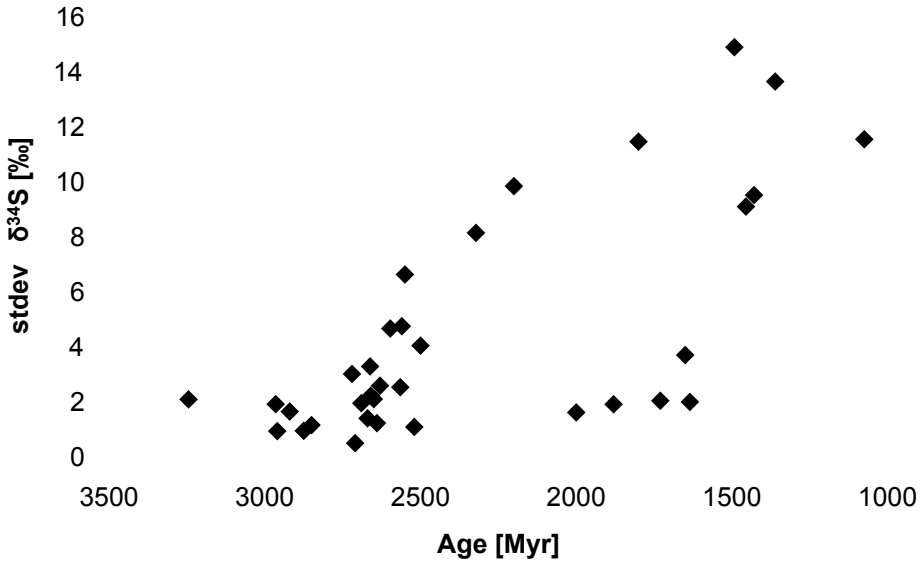

Fig. S4: Time-point standard deviation of $\delta^{34}S$ composition. See Table S1 for references.

S3.3. Deposition rate

The total weathering flux may be overestimated if the deposition rate D was smaller in the Precambrian than the Phanerozoic average used in the model. If continents increased in size over time, then this would mostly affect results for the mid Archaean. Thus by applying a constant, possibly too high, value for D throughout the Precambrian, the difference in $F_w(t)$ between the Archaean and the Proterozoic may in fact appear smaller than it actually was.

Most models of crustal growth (e.g. ref. 60) predict that continents had reached nearly 80 % of today's volume around the time of the GOE. Most recently, it was demonstrated using zircon data that 80 % of the present volume, as well as a modern style of crystal recycling, may already have been in place by 3 Gyr (refs. 69,70). It is thus unlikely that the long-term average deposition rate has changed drastically since the mid-Archaean. Furthermore, while using an adjusted deposition rate D changes the $F_w(t)/F_{volc}(t)$ ratio slightly (Table S2), but it does not significantly lower the importance of continental weathering as a source of sulphur to continental shelves. For the second Archaean stage (2.8-2.5 Gyr), the calculated ratio $F_w(t)/F_{volc}(t)$ is greater than unity for a deposition rate D down to $1.6 \cdot 10^{15}$ g yr^{-1}, or 36 % of the average Phanerozoic value. Flament *et al.*[71] estimated that until the end of the Archaean continents were mostly submerged and only 2-3 % of the Earth's surface area were above sea level based on a theoretical model. This scenario perhaps contradicts recent data[70], but if correct it may have resulted in a significantly lower value for D and a relatively higher contribution of volcanic sulphur to continental shelves. However, it is unlikely that the observed increases in total sulphur concentration at 2.8 Gyr and 2.5 Gyr were due to continental emergence alone, because that would also have raised the erosion rate of silicate minerals and not led to a selective increase in sulphur abundance. And for total sulphur concentration to increase by ~ 400 % at 2.8 Gyr (Table

S3) the sulphur weathering flux must have contributed a significant fraction to the total supply of sulphur to marine shelves. Hence even if the total weathering flux $F_w(t)$ were smaller in the Archaean than calculated with a constant value for D of $4.4 \cdot 10^{15}$ g yr^{-1}, the $F_w(t)/F_{volc}(t)$ was probably close to or greater than unity and weathering therefore an important source of sulphur to continental shelves.

It is likely that D varied regionally (*cf.* ref. 57) and temporally over the course of supercontinent cycles, which probably explains part of the variations in $F_w(t)$ (Fig. 1). However, the value of $4.4 \cdot 10^{15}$ g yr^{-1} calculated by Gregor[56] is an average over the entire Phanerozoic, which also experienced large fluctuations in total shelf area as eustatic sea-level changed and as super-continents amalgamated and broke up. It is therefore reasonable to use this value to calculate averages over several hundred million years.

Table S2: Effect of changing D on F_w/F_{volc} ratio.

	D = $3.5 \cdot 10^{15}$ g yr^{-1}	**D = $4.4 \cdot 10^{15}$ g yr^{-1}**
3.3-2.8 Gyr	0.2	0.4
2.8-2.5 Gyr	3.5	4.7
>2.5 Gyr	2.1	2.9
2.5-1.0 Gyr	10.6	13.6

S3.4. Reactant availability

Sulphur produced by oxidative biological or abiotic weathering on continents would have been in the form of sulphate. Permanent storage of sulphate in marine sediments prior to the advent of major evaporite depositories requires reduction to sulphide, with organic carbon acting as the major reducing agent. Reaction with iron then forms iron sulphide minerals. Hence the increase

in the total sulphur concentration of marine sediments over time (Fig. S1) could in theory also be controlled by an increase in the availability of organic carbon or reactive iron rather than an increase in the delivery of sulphate to the ocean.

Before the GOE, ferrous iron would have been delivered to the oceans by anoxic weathering of iron-rich rocks. This source would have been largely extinguished by atmospheric oxygenation. After the GOE, the major source of ferrous iron to the ocean was probably hydrothermal activity[72], which, similar to volcanic activity, probably decreased over time (*e.g.* ref. 59). It is therefore unlikely that reactive iron became more abundant across the Archaean-Proterozoic boundary and it can therefore not serve as an explanation for increasing sulphur concentrations in marine sediments.

Total organic carbon in marine sediments increases together with total sulphur (Fig. S5, Table S3), and the change for each from the Archaean to the Proterozoic is statistically significant (Table S4). However, the average S/TOC ratio remains nearly constant (Fig. S6, Table S3), and variations in S/TOC between the Archaean and Proterozoic are not statistically significant (Table S4). Hence if the organic carbon availability increased, it may have resulted in increased sulphide deposition on continental shelves, even if the flux of sulphate to the ocean remained constant. Organic carbon concentrations in marine sediments are controlled by (i) the redox state of the water column and hence the rate of remineralization, (ii) the availability of nutrients driving productivity, and (iii) the sedimentation rate. We comment on these in turn:

(i) It is unlikely that the redox state of the water column became more reduced from the Archaean into the Proterozoic, as atmospheric oxygen levels increased (*e.g.* ref. 65).

(ii) Nutrients would have been introduced by hydrothermal activity or continental weathering. The former likely decreased over time (Supplementary Section S2.2.), while the latter is in turn

tied to the delivery of sulphate to the ocean. In other words, the total sulphur concentration of marine sediments probably did not increase just because of higher concentrations of organic matter, but instead, productivity was probably stimulated by increasing weathering fluxes of sulphate and associated trace metals, many of which are micronutrients.

(iii) see Supplementary Section S2.3.

Table S3: Average total sulphur, total organic carbon (TOC) and S/TOC ratio.

	Total S [wt. %]	**TOC [wt. %]**	**S/TOC**
3.3-2.8 Gyr	0.12 ± 0.11	0.47 ± 0.67	1.11 ± 1.04
2.8-2.5 Gyr	0.49 ± 0.40	1.52 ± 1.33	1.14 ± 0.76
>2.5 Gyr	0.34 ± 0.36	1.11 ± 1.22	1.13 ± 0.85
2.5-1.0 Gyr	0.98 ± 1.00	2.07 ± 2.18	1.19 ± 1.30

Table S4: One-tailed p-values calculated with Student t-test, assuming unequal variance.

	Total sulphur	**TOC**	**S/TOC**
3.3-2.8 Gyr to 2.8-2.5 Gyr	0.002	0.011	0.474
2.8-2.5 Gyr to 2.5-1.0 Gyr	0.014	0.165	0.432
>2.5 Gyr to 2.5-1.0 Gyr	0.002	0.030	0.417

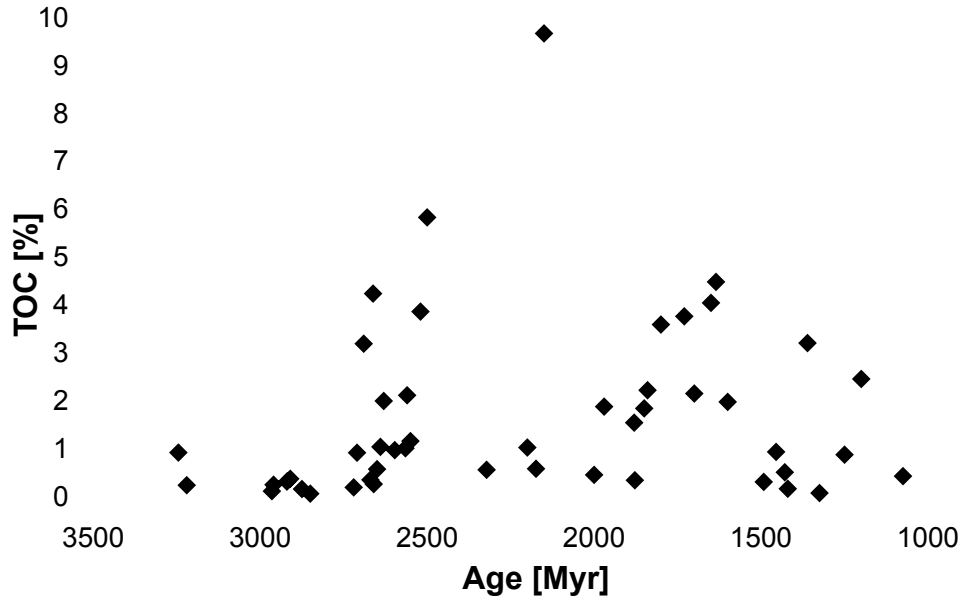

Fig. S5: Time-point average TOC concentrations. For references, see Table S1.

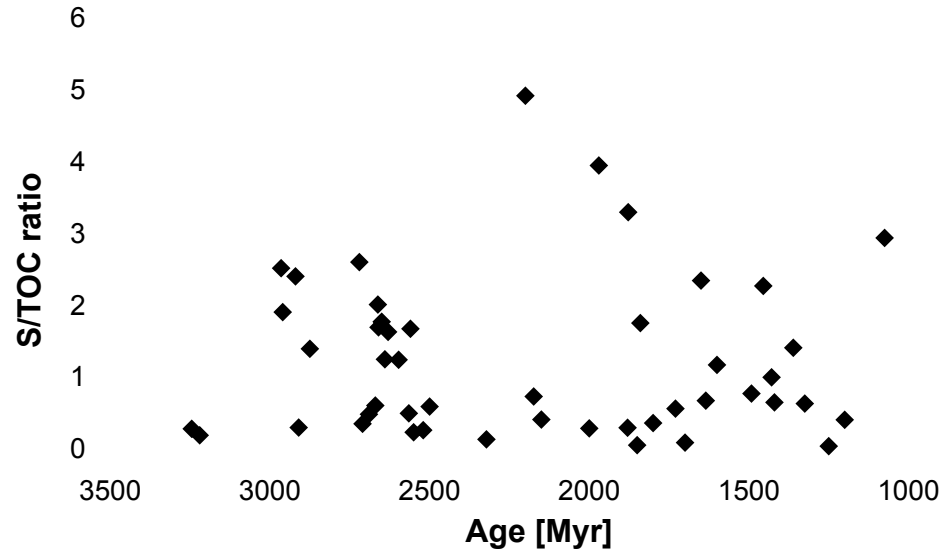

Fig. S6: Sulphur/TOC weight percent ratio over time. For references, see Table S1. (One outlier at 2850 Myr with an S/TOC ratio of 19.4 was removed. As can be seen from Figure S1 and S5 this outlier was most likely driven by an exceptionally low TOC concentration rather than a high total sulphur abundance).

S4. Possible biases in the biological and detrital flux

The calculated flux $F_{bioticw}(t) = F_w(t) - A_{py} \cdot R_{po2}$ could theoretically be biased by inaccuracies in each of the terms.

S4.1. Sensitivity to the total weathering flux

The biological and detrital flux $F_{bioticw}(t)$ may be overestimated if the calculated total weathering flux $F_w(t)$ is higher than in reality. As discussed above (Supplementary Section S3) the most likely bias in $F_w(t)$ might arise from applying the Phanerozoic average sedimentation rate to the Precambrian. Reducing the average sedimentation rate D to 80 % of the modern value (*cf.* Supplementary Section S3.3) while keeping all other parameters constant lowers the $F_{bioticw}(t)/F_{abioticw}(t)$ ratio (Table S5), but the abiotic weathering rate $F_{abioticw}(t)$ is still smaller for all time periods. If the Precambrian deposition rate, D, was smaller due to smaller continents, the same should have been true for the fraction of volcanic sulphur being deposited on continents and shelves (Supplementary Section S3.3) and for the total surface area of exposed pyrite, A_{py}. Hence the $F_{bioticw}(t)/F_{abioticw}(t)$ ratio would probably have been comparatively insensitive to continental area. As $F_{abioticw}(t)$ is perhaps more likely to be overestimated (see below), we conclude that even if D was smaller in the Precambrian and all other parameters remained constant, a detrital and/or biological sulphur flux would still have been necessary to explain the observed concentrations of sulphur in marine sediments.

Table S5: Effects of changes in D on the $F_{bioticw}(t)/F_{abioticw}(t)$ ratio.

	D = $4.4 \cdot 10^{15}$ g yr^{-1}	**D = $3.5 \cdot 10^{15}$ g yr^{-1}**
3.3-2.8 Gyr	14.7	5.7
2.5-2.8 Gyr	155.9	85.8
>2.5 Gyr	100.7	54.5
1.0-2.5 Gyr	2.6	1.1

S4.2. Total exposed surface area of pyrite

If the total surface area of pyrite exposed to weathering (A_{py}) is overestimated, then this would result in an underestimation of $F_{bioticw}(t)$, given the way that abiotic weathering depends on A_{py}. In our model, we initially assume that all of the pyrite weathered today is subject to abiotic weathering, because the proportions of biological and abiotic weathering are unknown. By subtracting the Proterozoic biogenic flux in five iterations (Supplementary Section 3.2.2), this assumption is essentially modified to 55 % of today's pyrite being oxidized abiotically. That is equivalent to 27.5 % of the total modern river flux being caused by abiotic pyrite oxidation, 22.5 % being caused by biotic pyrite oxidation, and the remaining 50 % being caused by sulfate dissolution or anthropogenic activity. These figures would imply that today the biological oxidation rate is nearly the same or somewhat smaller than the abiotic oxidation rate. However, experimental work has shown that especially under low pH conditions the biological pyrite oxidation rate is several orders of magnitude higher than the abiotic oxidation rate (reviewed in ref. 73). This is because oxidation of pyrite results in acidification of the weathering solution and the abiotic oxidation rate declines with decreasing pH (*cf.* ref. 63,64, Supplementary Section S4.3). Our estimate of A_{py} is therefore more likely to be too high, meaning that abiotic oxidation (eq. S8) is probably overestimated so that $F_{bioticw}(t)$ (eq. S10) is underestimated, if anything, so that our conclusion of a late Archaean biotic flux is unmodified. Table S6 shows how our calculated ratio of biotic to abiotic weathering in the Precambrian changes if the fraction of modern abiotic oxidation (K) is modified. Even if 50 % of the modern river flux were due to natural abiotic oxidation of pyrite, the biotic oxidation of pyrite would still have been of similar magnitude as abiotic oxidation in the Proterozoic, and biotic oxidation would be necessary to

explain the late Archean weathering flux irrespective of *K*. A value greater than 50 % for *K* is unlikely not only because of the known effects of biological activity, but also because of the known contributions of sulfate dissolution and anthropogenic mining activities, which together make up more than 50 % of the total modern river flux[51].

Table S6: $F_{bioticw}/F_{abioticw}$ as a function of *K*. Here *K* is defined as the fraction of the modern river flux[66] that is caused by abiotic oxidation of pyrite.

K	10%	30%	50%	70%	90%	100%
2.5-1.0 Gyr	8.9	2.3	1.0	0.4	0.1	0.0
> 2.5 Gyr	279.4	92.5	55.1	39.1	30.2	27.0
3.3-2.8 Gyr	42.4	13.5	7.7	5.2	3.8	3.3
2.8-2.5 Gyr	431.7	143.2	85.5	60.8	47.1	42.3

S4.3. Oxidation rate

The oxidation rate determined by Williamson and Rimstidt[61] is a function of pH (Fig. S7). We use pH = 7 as a conservative estimate in our model, but it is possible that the oxidation of pyrite occurred in more acidic environments, because atmospheric CO_2 concentrations were probably higher in the Precambrian resulting in more acidic rain water (ref. 74 and references therein). Furthermore, acidity is generated during the oxidation itself (*e.g.* ref. 63,64). At pH 4, for example, the oxidation rate would be smaller by a factor of 2.1 compared to pH 7 (Fig. S7). If weathering fluids in the Precambrian were significantly more acidic than they are today, the calculated $F_{bioticw}/F_{abioticw}$ ratio would be higher. The values presented in Table S5 of $F_{bioticw}/F_{abioticw}$ are thus probably an underestimation.

Uncertainties in the exponents of the rate law (Eq. S7) could lower or raise the calculated abiotic oxidation rate by several percent (Fig. S8). In most cases, the errors in the exponents to pH and pO_2 have negligible effects, reaching 25 % only under low O_2 and neutral pH conditions. Uncertainties in the first factor of Eq. S7 can alone impart errors of up to 25 %. In the most extreme case this could result in a total uncertainty of up to 60 % for the abiotic weathering rate, but even then the biogenic or detrital weathering flux of sulphur would still be much larger (see Fig. 2).

It is possible that the rate law determined by Williamson and Rimstidt[61] is not always applicable under natural conditions. For example, the presence of $Fe^{3+}_{(aq)}$ is known to increase the abiotic weathering rate[61]. However, the scarcity of ferric iron minerals in paleosols until ~2.4 Gyr and the stability of ferrous iron at the Earth's surface[65] suggest that $Fe^{3+}_{(aq)}$ was probably not generated at large quantities to abiotically oxidize significant quantities of pyrite in the late Archaean. Furthermore, as discussed by Konhauser et al.[64], the reaction between pyrite and $Fe^{3+}_{(aq)}$ is not self-sustaining and will stop if $Fe^{3+}_{(aq)}$ is not regenerated by oxidation of Fe^{2+} with O_2. Another thermodynamically possible oxidant is Mn^{4+} (ref.75); however, due to its high redox potential the production of Mn^{4+} from Mn^{2+} is likely too slow[64]. Also NO_3^- can serve as an oxidant for sulphide[76]; however, the modeled flux of NO_3^- from the atmosphere to the Earth's land surface in the late Archaean[77] is one order of magnitude smaller than the total weathering flux of sulphur and therefore also abiotic NO_3^- alone could not have been the major oxidant. Pyrite oxidation is thus ultimately dependent on molecular oxygen and we therefore adopt the pO_2-dependent rate law.

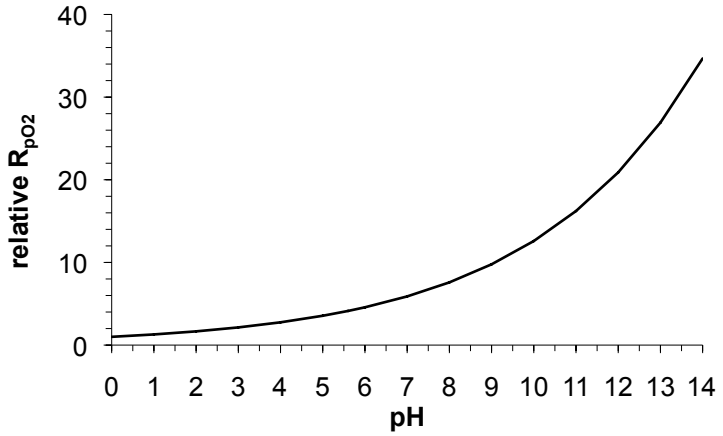

Fig. S7: Change in abiotic oxidation rate R_{pO2} as a function of pH, relative to pH = 0 (Eq. S7).

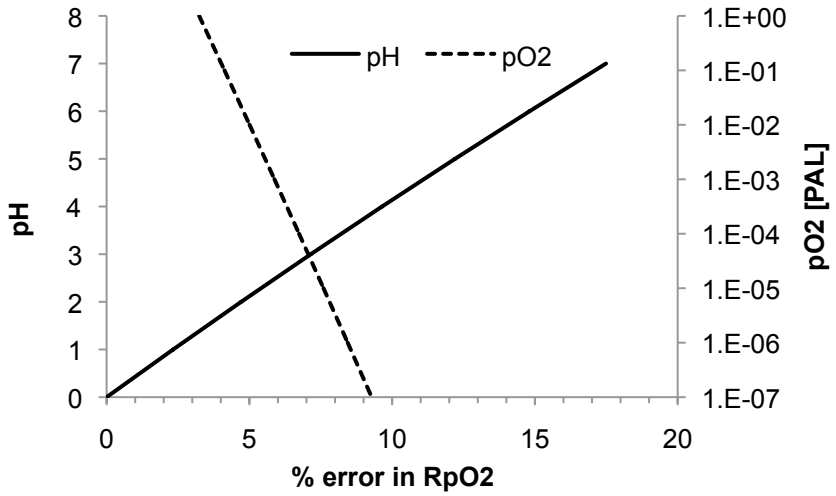

Fig. S8: Percent error in R_{pO2} arising by reducing the exponent of either pH or pO_2 by 1 sigma (Eq. S7). (Results for addition of 1 sigma are within ± 1 % of these values).

S5. Analysis of bias in temporal subdivisions around 2.5 Gyr and 2.8 Gyr

The analysis of the data may be biased by *a priori* assumptions about major transitions in the redox state of the Earth's atmosphere. To test that, we divided the $F_w(t)$ data set (Fig. 1) at

various time points and calculated the statistical significance of the difference in $F_w(t)$ between the resulting data blocks (Fig. S9). By far the lowest p-values were obtained for divisions at 2.8 Gyr ($p = 2.6 \cdot 10^{-6}$) and 2.7 Gyr ($p = 6.2 \cdot 10^{-6}$), which coincides with the time when a wider spread in $\delta^{34}S$ values of marine sedimentary sulphides indicates locally increased seawater sulphate concentrations[7]. The p-value exceeds 0.01 (*i.e.* the 99 % confidence limit is no longer met) for all divisions at ages younger than 2.5 Gyr and it generally increases with decreasing division ages (Fig. S9). Since 2.5 Gyr is roughly the beginning of the Great Oxidation Event, we conclude that the observed changes in the total weathering flux ($F_w(t)$, Fig. 1) are predominantly driven by global increases in atmospheric oxygen and that therefore our chosen boundaries at 2.8 Gyr and 2.5 Gyr are not arbitrary.

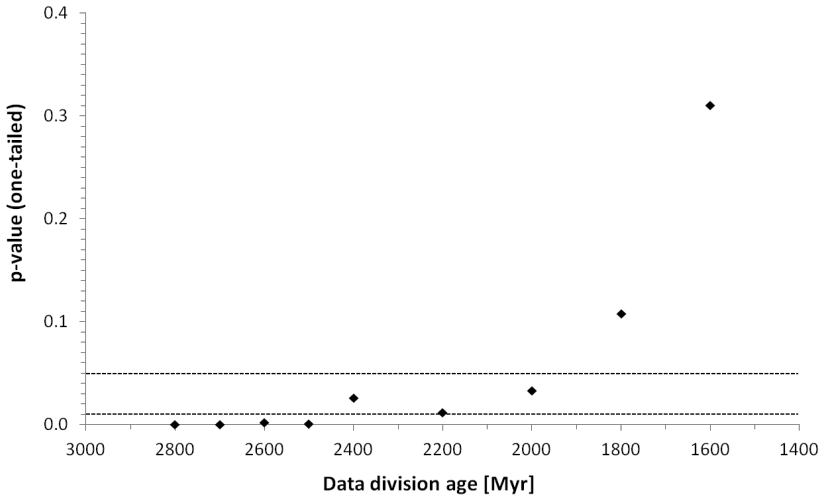

Fig. S9: Student t-test results for divisions of the data set at various ages. Dashed lines indicate 95 % and 99 % confidence levels.

S6. Agreement with other proxies

Our conclusion that oxidative weathering aided by microbial activity began in the late Archean is supported by other independent evidence. Konhauser et al.[64] concluded that Cr abundances indicate oxidative weathering started during the GOE because the largest enrichment in Cr

occurs between 2.48 and 2.32 Gyr (Fig. S10). However, Cr has a higher redox potential than sulphur, and hence their data are thus not inconsistent with late Archaean oxidative weathering commencing before 2.5 Gyr, but in fact support the second rise in S weathering observed around 2.5 Gyr.

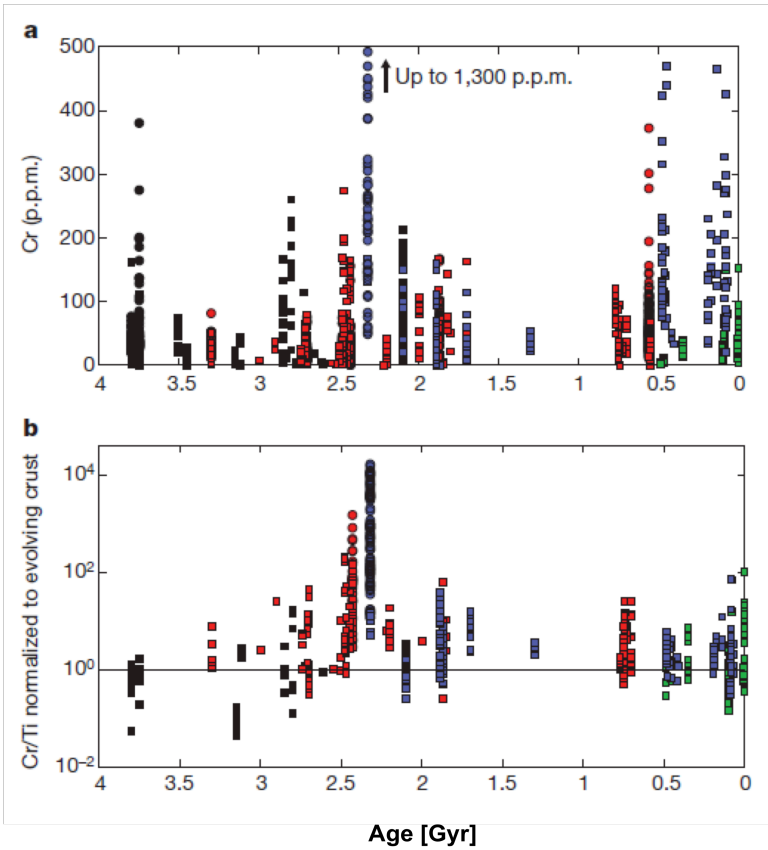

Fig. S10: Chromium abundances in marine iron oxide deposits over time (taken from ref. 64). Black marks Algoma-type iron formations (may be subject to volcanic Cr-enrichment), red marks Superior-type iron formations (form on continental shelves), blue marks oolitic iron stones (shallow water), green marks Phanerozoic hydrothermal and exhalative iron formations.

Another commonly used proxy for oxidative weathering is the total concentration of molybdenum, or the Mo/TOC ratio. We have augmented the existing Mo database[2] with published data from the earlier Archaean (Fig. S11), and the results show that Mo concentrations in marine sediments began to increase in the 2.8-2.7 Gyr interval.

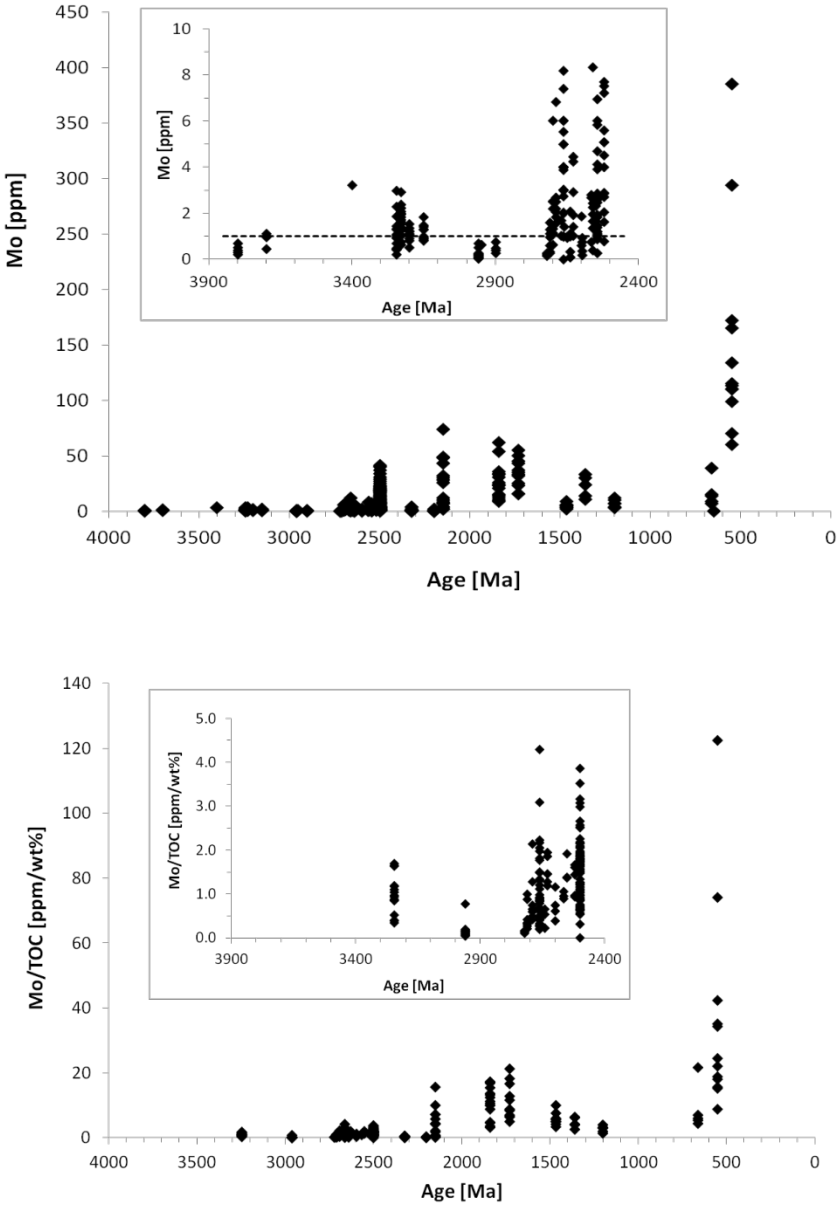

Fig. S11: Total Mo (top) and Mo/TOC ratios (bottom) in marine sediments (clastics and chert) through the Precambrian. Inserts show Archaean data only, where the Mt. McRae Shale data (0.2-41.4 ppm (ref. 78) is excluded from the insert in the top panel for better scale. Data are taken from refs. 2,26,78-83. Dashed line marks the modern crustal average[83].

Lastly, the record of mass-dependent sulphur isotope fractionation (Fig. S12) is consistent with increasing levels of sulphate in the ocean starting between 2.8-2.7 Gyr (*cf.* ref. 7), when values begin to show a broader spread and a significant difference between sulphides and sulphates at

that time. Both features are indicative of bacterial sulphate reduction with marine sulphate concentrations larger than 1 % modern levels[68].

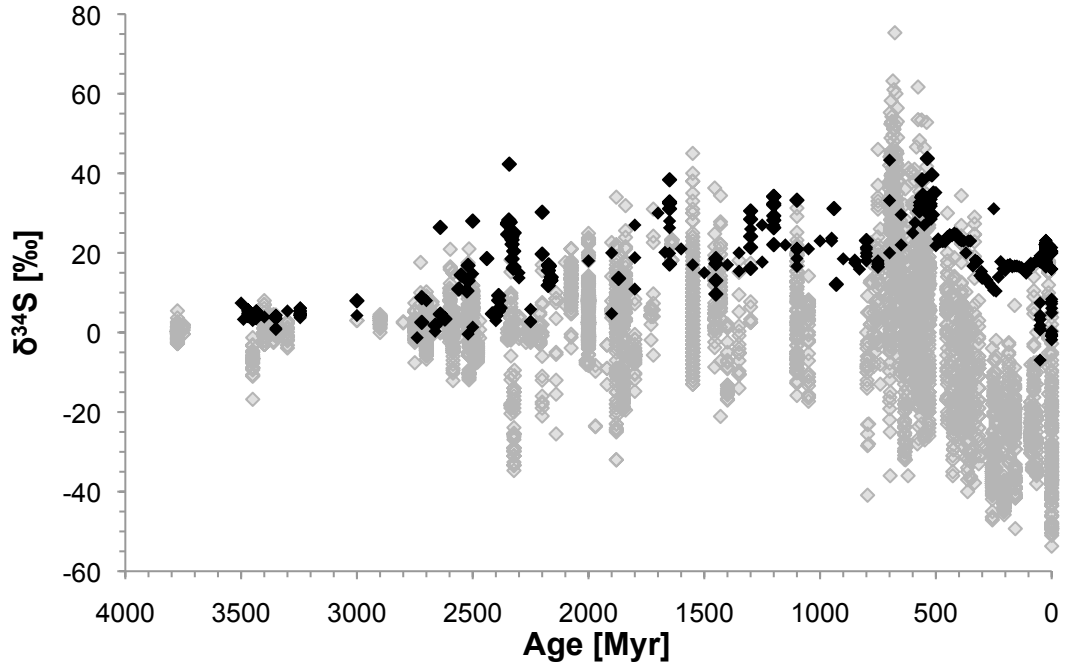

Fig. S12: Mass-dependent sulphur isotope record from marine sediments. Black diamonds are sulphates[24,47,84-90], gray diamonds are sulphides[55].

References

[1] Burnie, S.W., Schwarcz, H.P., & Crocket, J.H., A sulfur isotopic study of the Whie Pine Mine, Michigan. *Econ. Geol.* **67 (7),** 895-914 (1972).

[2] Scott, C.T. *et al.*, Tracing the stepwise oxygenation of the Proterozoic ocean. *Nature* **452,** 456-459 (2008).

[3] Strauss, H. & Moore, T.B., Abundances and isotopic compositions of carbon and sulfur species in whole rock and kerogen samples in *The Proterozoic Biosphere - A Multidisciplinary Study*, edited by J.W. Schopf & C. Klein (Cambridge University Press, Cambridge, 1992).

[4] Donnelly, T.H., Depositional environment of the middle Proterozoic Velkerri Formation in northern Australia: geochemical evidence. *Precambrian Res.* **42,** 165-172 (1988).

[5] Johnston, D.T. *et al.*, Sulfur isotope biogeochemistry of the Proterozoic McArthur Basin. *Geochim. Cosmochim. Ac.* **72,** 4278-4290 (2008).

[6] Jackson, M.J. & Raiswell, R., Sedimentoogy and carbon-sulphur geochemistry of the Velkerri Formation, a mid-Proterozoic potential oil source in northern Australia. *Precambrian Res.* **54,** 81-108 (1991).

[7] Strauss, H., The isotopic composition of Precambrian sulphides - seawater chemistry and biological evolution in *Precambrian Sedimentary Environments: A Modern Approach to Ancient Depositional Systems*, edited by W. Altermann & P.L. Corcoran (Blackwell Science, Oxford, 2002).

[8] Australian Stratigraphic Units Database, http://www.ga.gov.au/products-services/data-applications/reference-databases/stratigraphic-units.html (Australian Government, 2011).

[9] Lyons, T.W., Luepke, J.J., Schreiber, M.E., & Zieg, G.A., Sulfur geochemical constraints on Mesoproterozoic restricted marine deposition: lower Belt Supergroup, northwestern United States. *Geochim. Cosmochim. Ac.* **64 (3),** 427-437 (2000).

[10] Banerjee, S., Dutta, S., Paikaray, S., & Mann, U., Stratigraphy, sedimentology and bulk organic geochemistry of black shales from the Proterozoic Vindhyan Supergroups (central India). *J. Earth Syst. Sci.* **115 (1),** 37-47 (2006).

[11] Shen, Y., Canfield, D.E., & Knoll, A.H., Middle Proterozoic ocean chemistry: Evidence from the McArthur Basin, Northern Australia. *Am. J. Sci.* **302,** 81-109 (2002).

[12] Planavsky, N.J. *et al.*, Widespread iron-rich conditions in the mid-Proterozoic ocean. *Nature* **477,** 448-451 (2011).

[13] Cameron, E.M. & Garrels, R.M., Geochemical composition of some Precambrian shales from the Canadian Shield. *Chem. Geol.* **28,** 181-197 (1980).

[14] Evangelatos, J., Butler, K., & Spray, J.G., A marine magnetic study of a carbonate-hosted impact structure: Ile Rouleau, Canada. *Geophys. J. Int.* **179 (1),** 171-181 (2009).

[15] Poulton, S.W., Fralick, P.W., & Canfield, D.E., The transition to a sulphidic ocean ~1.84 billion years ago. *Nature* **431,** 173-177 (2004).

[16] Medvedev, P.V., Melezhik, V.A., & Filippov, M.M., Paleoproterozoic petrified oil field (Shunga Event). *Paleontol. J.* **43 (8),** 972-979 (2009).

[17] Johnston, D.T. *et al.*, Evolution of the oceanic sulfur cycle at the end of the Paleoproterozoic. *Geochim. Cosmochim. Ac.* **70 (23),** 5723-5739 (2006).

[18] Findlay, J.M., Parrish, R.R., Birkett, T.C., & Watanabe, D.H., U-Pb ages from the Nimish Formation and Montagnais glomeroporphyritic gabbro of the central New Quebec Orogen, Canada. *Can. J. Earth Sci.***32 (8),** 1208-1220 (1995).

[19] Zentmyer, R.A., Pufahl, P.K., James, N.P., & Hiatt, E.E., Dolomitization on an evaporitic Paleoproterozoic ramp: Widespread synsedimentary dolomite in the Denault Formation, Labrador Trough, Canada. *Sediment. Geol.* **238 (1-2),** 116-131 (2011).

[20] Hoffman, P.F., Bowring, S.A., Buchwaldt, R., & Hildebrand, R.S., Birthdate for the Coronation paleocean: age of initial rifting in Wopmay orogen, Canada. *Can. J. Earth Sci.***48 (2),** 281-293 (2011).

[21] Melezhik, V.A., Grinenko, L.N., & Fallick, A.E., 2000-Ma sulphide concretions from teh 'Productive' Formation of the Pechenga Greenstone Belt, NW Russia: genetic history based on morphological and isotopic evidence. *Chem. Geol.* **148,** 61-94 (1998).

[22] Kuznetsov, A.B. *et al.*, Rb-Sr and U-Pb systematics of metasedimentary carbonate rocks: The Paleoproterozoic Kuetsjarvi Formation of the Pechenga Greenstone Belt, Kola Peninsula. *Lithol. Miner. Resour.* **46 (2),** 151-164 (2011).

[23] Watanabe, Y., Naraoka, H., Wronkiewicz, D.J., Condie, K.C., & Ohmoto, H., Carbon, nitrogen, and sulfur geochemistry of Archean and Proterozoic shales from the Kaapvaal Craton, South Africa. *Geochim. Cosmochim. Ac.* **61 (16),** 3441-3459 (1997).

[24] Guo, Q. *et al.*, Reconstructing Earth's surface oxidation across the Archean-Proterozoic transition. *Geology* **37 (5),** 399-402 (2009).

[25] Strauss, H. & Beukes, N.J., Carbon and sulfur isotopic compositions of organic carbon and pyrite in sediments from the Transvaal Supergroup, South Africa. *Precambrian Res.* **79,** 57-71 (1996).

[26] Yamaguchi, K.E., Pennsylvania State Univeristy, 2002.

[27] Bekker, A. *et al.*, Dating the rise of atmospheric oxygen. *Nature* **427,** 117-120 (2004).

[28] Papineau, D., Mojzsis, S.J., & Schmitt, A.K., Multiple sulfur isotopes from Paleoproterozoic Huronian interglacial sediments and the rise of atmospheric oxygen. *Earth Planet. Sc. Lett.* **255 (1-2),** 188-212 (2007).

[29] Cameron, E.M., Genesis of Proterozoic iron-formation: sulphur isotope evidence. *Geochim. Cosmochim. Ac.* **47,** 1069-1074 (1983).

[30] Pickard, A.L., SHRIMP U–Pb zircon ages for the Palaeoproterozoic Kuruman Iron Formation, Northern Cape Province, South Africa: evidence for simultaneous BIF deposition on Kaapvaal and Pilbara Cratons. *Precambrian Res.* **125 (3-4),** 275-315 (2003).

[31] Simonson, B.M., Sumner, D.Y., Beukes, N.J., Johnson, S., & Gutzmer, J., Correlating multiple Neoarchean-Paleoproterozoic impact spherule layers between South Africa and Western Australia. *Precambrian Res.* **169,** 100-111 (2009).

[32] Kaufman, A.J. *et al.*, Late Archean biospheric oxygenation and atmospheric evolution. *Science* **317,** 1900-1903 (2007).

[33] Ono, S. *et al.*, New insights into Archean sulfur cycle from mass-independent sulfur isotope records from the Hamersley Basin, Australia. *Earth Planet. Sc. Lett.* **213,** 15-30 (2003).

[34] Ono, S., Beukes, N.J., & Rumble III, D., Origin of two distinct multiple-sulfur isotope compositions of pyrite in the 2.5 Ga Klein Naute Formation, Griqualand West Basin, South Africa. *Precambrian Res.* **169,** 48-57 (2009).

[35] Sumner, D.Y. & Beukes, N.J., Sequence stratigraphic development of the Neoarchean Transvaal cabonate platform, Kaapvaal Craton, South Africa. *S. Afr. J. Geol.***109,** 11-22 (2009).
[36] Bumby, A.J., Eriksson, K.A., Catuneanu, O., Nelson, D.R., & Rigby, M.J., Meso-Archaean and Palaeo-Proterozoic sedimentary sequence stratigraphy of the Kaapvaal Craton. *Mar. Petrol. Geol.* **33 (1)**, 92-116 (2012).
[37] Ono, S., Kaufman, A.J., Farquhar, J., Sumner, D.Y., & Beukes, N.J., Lithofacies control on multiple-sulfur isotope records and Neoarchean sulfur cycles. *Precambrian Res.* **169,** 58-67 (2009).
[38] Czaja, A.D. *et al.*, Iron and carbon isotope evidence for ecosystem and environmental diversity in the ~2.7 to 2.5 Ga Hamersley Province, Western Australia. *Earth Planet. Sc. Lett.* **292,** 170-180 (2010).
[39] Partridge, M.A., Golding, S.D., Baublys, K.A., & Young, E., Pyrite paragenesis and multiple sulfur isotope distribution in late Archean and early Paleoproterozoic Hamersley Basin sediments. *Earth Planet. Sc. Lett.* **272 (1-2),** 41-49 (2008).
[40] Rasmussen, B., Blake, T.S., & Fletcher, I.R., U-Pb zircon age constraints on the Hamersley spherule beds: Evidence for a single 2.63 Ga Jeerinah-Carawine impact ejecta layer *Geology* **33 (9),** 725-728 (2005).
[41] Kakegawa, T., Kasahara, Y., Hayashi, K.-I., & Ohmoto, H., Sulfur and carbon isotope analyses of the 2.7 Ga Jeerinah Formation, Fortescue Group, Australia. *Geochem. J.* **34,** 121-133 (2000).
[42] Scott, C.T. *et al.*, Late Archean euxinic conditions before the rise of atmospheric oxygen. *Geology* **39 (2),** 119-122 (2011).
[43] Farquhar, J. *et al.*, Isotopic evidence for Mesoarchaean anoxia and changing atmospheric sulphur chemistry. *Nature* **449,** 706-709 (2007).
[44] Ohmoto, H., Watanabe, Y., Ikemi, H., Poulson, S.R., & Taylor, B.E., Sulphur isotope evidence for an oxic Archaean atmosphere. *Nature* **442,** 908-911 (2006).
[45] Ono, S., Beukes, N.J., Rumble III, D., & Fogel, M.L., Early evolution of atmospheric oxygen from multiple-sulfur and carbon isotope records of the 2.9 Ga Mozaan Group of the Pongola Supergroup, South Africa. *S. Afr. J. Geol.***109,** 97-108 (2006).
[46] Holland, H.D., *The chemical evolution of the atmosphere and oceans*. (Princeton University Press, Princeton, NJ, 1984).
[47] Bao, H., Rumble III, D., & Lowe, D.R., The five stable isotope compositions of Fig Tree barites: Implications on sulfur cycle in ca. 3.2 Ga oceans. *Geochim. Cosmochim. Ac.* **71 (20),** 4868-4879 (2007).
[48] Javaux, E.J., Marshall, C.P., & Bekker, A., Organic-walled microfossils in 3.2-billion-year-old shallow-marine siliciclastic deposits. *Nature* **463,** 934-938 (2010).
[49] Schopf, J.W., Kudryavtsev, A.B., Czaja, A.D., & Tripathi, A.B., Evidence of Archean life: Stromatolites and microfossils. *Precambrian Res.* **158 (3-4),** 141-155 (2007).
[50] Holland, H.D., Lazar, B., & McCaffrey, M., Evolution of the atmosphere and oceans. *Nature* **320,** 27-33 (1986).
[51] Berner, E.K. & Berner, R.A., *The global water cycle - geochemistry and environment*. (Prentice-Hall, Inc., Englewood Cliffs, NJ, 1987).
[52] Farquhar, J., Wu, N., Canfield, D.E., & Oduro, H., Connections between sulfur cycle evolution, sulfur isotopes, sediments, and base metal sulfide deposits. *Econ. Geol.* **105,** 509-533 (2010).

[53] Canfield, D.E. & Teske, A., Late Proterozoic rise in atmospheric oxygen concentration inferred from phylogenetic and sulphur-isotope studies. *Nature* **382,** 127-132 (1996).
[54] Kah, L.C., Lyons, T.W., & Frank, T.D., Low marine sulphate and protracted oxygenation of the Proterozoic biosphere. *Nature* **431,** 834-838 (2004).
[55] Canfield, D.E. & Farquhar, J., Animal evolution, bioturbation, and the sulfate concentration of the oceans. *P. Natl. Acad. Sci.* **106 (20),** 8123-8127 (2009).
[56] Gregor, C.B., The mass-age distribution of Phanerozoic sediments in *The chronology of the geologic record*, edited by N.J. Snelling (The Geological Society of London, London, UK, 1985), Vol. 10, pp. 284-289.
[57] Garrels, R.M. & Mackenzie, F.T., *Evolution of sedimentary rocks*. (W. W. Norton & Company. Inc., New York, 1971).
[58] Poulton, S.W. & Canfield, D.E., Ferruginous conditions: A dominant feature of the ocean through Earth's history. *Elements* **7,** 107-112 (2011).
[59] Canfield, D.E., The evolution of the Earth surface sulfur reservoir. *Am. J. Sci.* **304,** 839-861 (2004).
[60] Eriksson, P.G., Sea level changes and the continental freeboard concept: general principles and application to the Precambrian. *Precambrian Res.* **97,** 143-154 (1999).
[61] Williamson, M.A. & Rimstidt, J.D., The kinetics and electrochemical rate-determining step of aqueous pyrite oxidation. *Geochim. Cosmochim. Ac.* **58 (24),** 5443-5454 (1994).
[62] Stumm, W. & Morgan, J.J., *Aquatic Chemistry*, 3rd ed. (John Wiley & Sons Inc., New York, 1996).
[63] Rohwerder, T. & Sand, W., Mechanisms and biochemical fundamentals of bacterial metal sulfide oxidation in *Microbial processing of metal sulfides*, edited by E.R. Donati & W. Sand (Springer, 2007), pp. 35-58.
[64] Konhauser, K.O. *et al.*, Aerobic bacterial pyrite oxidation and acid rock drainage during the Great Oxidation Event. *Nature* **478,** 369-373 (2011).
[65] Catling, D.C. & Claire, M.W., How Earth's atmosphere evolved to an oxic state: a status report. *Earth Planet. Sc. Lett.* **237,** 1-20 (2005).
[66] Emerson, S. & Hedges, J., *Chemical oceanography and the marine carbon cycle*. (Cambridge University Press, Cambridge, UK, 2008).
[67] Holland, H.D., When did the Earth's atmosphere become oxic? A Reply. *Geochem. News* **100,** 20 (1999).
[68] Habicht, K.S., Gade, M., Thamdrup, B., Berg, P., & Canfield, D.E., Calibration of sulfate levels in the Archean Ocean. *Science* **298,** 2372-2374 (2002).
[69] Hawkesworth, C.J. *et al.*, The generation and evolution of the continental crust. *J. Geol. Soc.* **167 (2),** 229-248 (2010).
[70] Dhuime, B., Hawkesworth, C.J., Cawood, P.A., & Storey, C.D., A change in the geodynamics of continental growth 3 billion years ago. *Science* **335,** 1334-1336 (2012).
[71] Flament, N., Coltice, N., & Rey, P.F., A case for late-Archaean continental emergence from thermal evolution models and hypsometry. *Earth Planet. Sc. Lett.* **275,** 326-336 (2008).
[72] Veizer, J., Compston, W., Hoefs, J., & Nielsen, H., Mantle buffering of the early oceans. *Naturwissenschaften* **69 (4),** 173-180 (1982).
[73] Roden, E.E., Microbiological controls on geochemical kinetics 2: Case study on microbial oxidation of metal sulfide minerals and future prospects in *Kinetics of water-*

rock interaction, edited by S.L. Brantley, J.D. Kubicki, & A.F. White (Springer, 2008), pp. 417-467.

[74] Fabre, S., Berger, G., & Nedelec, A., Modeling of continental weathering under high-CO2 atmospheres during Precambrian times. *Geochem. Geophy. Geosy.* **12 (10),** doi:10.1029/2010GC003444 (2011).

[75] Bottrell, S.H. *et al.* Abiotic sulfide oxidation via manganese fuels the deep biosphere: stable isotope evidence in *EGU General Assembly* (Geophysical Research Abstracts, 2008), Vol. 10, pp. EGU2008-A-10613.

[76] Bosch, J., Lee, K.-Y., Jordan, G., Kim, K.-W., & Meckenstock, R.U., Anaerobic, Nitrate-Dependent Oxidation of Pyrite Nanoparticles by Thiobacillus denitrificans. *Envir. Sci. Tech.* **46 (4),** 2095-2101 (2012).

[77] Ducluzeau, A.-L. *et al.*, Was nitric oxide the first deep electron sink? *TRENDS Biochem. Sci.* **34 (1),** 9-15 (2008).

[78] Anbar, A. *et al.*, A whiff of oxygen before the Great Oxidation Event? *Science* **317 (5846),** 1903-1906 (2007).

[79] McLennan, S.M., Taylor, S.R., & Eriksson, K.A., Geochemistry of Archean shales from the Pilbara Supergroup, Western Australia. *Geochim. Cosmochim. Ac.* **47,** 1211-1222 (1983).

[80] McLennan, S.M., Taylor, S.R., & Kroener, A., Geochemical evolution of Archean shales from South Africa. I. The Swaziland and Pongola Supergroups. *Precambrian Res.* **22,** 93-124 (1983).

[81] McLennan, S.M., Taylor, S.R., & McGregor, V.R., Geochemistry of Archean metasedimentary rocks from West Greenland. *Geochim. Cosmochim. Ac.* **48,** 1-13 (1984).

[82] Siebert, C., Kramers, J.D., Meisel, T., Morel, P., & Naegler, T.F., PGE, Re-Os, and Mo isotope systematics in Archean and early Proterozoic sedimentary systems as proxies for redox conditions of early Earth. *Geochim. Cosmochim. Ac.* **69 (7),** 1787-1801 (2005).

[83] Wille, M. *et al.*, Evidence for a gradual rise of oxygen between 2.6 and 2.5 Ga from Mo isotopes and Re-PGE signatures in shales. *Geochim. Cosmochim. Ac.* **71,** 2417-2435 (2007).

[84] Domagal-Goldman, S.D., Kasting, J.F., Johnston, D.T., & Farquhar, J., Organic haze, glaciations and multiple sulfur isotopes in the Mid-Archean Era. *Earth Planet. Sc. Lett.* **269,** 29-40 (2008).

[85] Farquhar, J., Bao, H., & Thiemens, M.H., Atmospheric influence of Earth's earliest sulfur cycle. *Science* **289,** 756-758 (2000).

[86] Farquhar, J. *et al.*, Mass-Independent Sulfur of Inclusions in Diamond and Sulfur Recycling on Early Earth. *Science* **298,** 2369-2372 (2002).

[87] Philippot, P. *et al.*, Early Archaean microorganisms preferred elemental sulfur, not sulfate. *Science* **317,** 1534-1537 (2007).

[88] Shen, Y., Farquhar, J., Masterson, A.L., Kaufman, A.J., & Buick, R., Evaluating the role of microbial sulfate reduction in the early Archean using quadruple isotope systematics. *Earth Planet. Sc. Lett.* **279,** 383-391 (2009).

[89] Ueno, Y., Ono, S., Rumble III, D., & Maruyama, S., Quadruple sulfur isotope analysis of ca. 3.5 Ga Dresser Formation: New evidence for microbial sulfate reduction in the early Archean. *Geochim. Cosmochim. Ac.* **72,** 5675-5691 (2008).

[90] Johnston, D.T. *et al.*, Active microbial sulfur disproportionation in the Mesoproterozoic. *Science* **310,** 1477-1479 (2005).